Available online at www.sciencedirect.com
ScienceDirect
Journal of Sound and Vibration 314 (2008) 650–656
JOURNAL OF SOUND AND VIBRATION
www.elsevier.com/locate/jsvi

Element size and time step selection procedures for the numerical analysis of elasticity with higher-order inertia

Harm Askes*, Beibei Wang, Terry Bennett

Department of Civil and Structural Engineering, University of Sheffield, Mappin Street, Sheffield S1 3JD, UK

Received 24 September 2007; received in revised form 13 December 2007; accepted 19 December 2007
Handling Editor: C. Morfey
Available online 4 February 2008

Abstract

Continuum theories with additional higher-order inertia terms have been suggested in the literature in order to be able to describe dispersive wave propagation and in order to include microstructural information in the macroscopic model. In this short note, we investigate two numerical discretisation aspects of such a model. Firstly, the critical time step is derived which is relevant for conditionally stable time integrators. Secondly, a discrete dispersion analysis is carried out by which the accuracy of the discretised model can be assessed a priori. Recommendations for the finite element size and the time step size can thus be made.

1. Introduction

In this short note, we discuss a few numerical discretisation aspects of continuum elasticity theories that are equipped with additional inertia terms. Denoting the space and time derivatives by a dash and a dot, respectively, the 1D-version of such a model can be written as

$$\rho\ddot{u} - \ell^2 \rho\, \ddot{u}'' = E\, u'', \tag{1}$$

where ρ and E are the mass density and the Young's modulus, u is the displacement and the additional inertia term is accompanied by the material length scale parameter ℓ that is a representation of the underlying microstructure of the material. The motivation for using Eq. (1) is often a more accurate simulation of dispersive wave propagation. Whereas classical elasticity theories without additional inertia are non-dispersive, experimental evidence reveals that the angular frequency of the higher wave numbers is normally lower than predicted by classical elasticity.

Although the above discussion may suggest otherwise, a solid microstructural background for the length scale parameter ℓ can be obtained. Especially the following procedure has been explored by many researchers,

*Corresponding author.
E-mail address: h.askes@sheffield.ac.uk (H. Askes).

0022-460X/$ - see front matter © 2008 Elsevier Ltd. All rights reserved.
doi:10.1016/j.jsv.2007.12.034

see for instance Refs. [1–3]:

- starting from a discrete or heterogeneous description of the material, continualisation or homogenisation principles are applied by which equivalent homogeneous continuum theories can be derived. If accuracy is desired beyond the leading order terms, normally a higher-order stiffness term is obtained, e.g. in the spirit of Eq. (1)

$$\rho\ddot{u} = E\,u'' + \ell^2\,E\,u''''. \tag{2}$$

- The higher-order stiffness term in Eq. (2) is unfortunately destabilising and in numerical simulations it would require additional continuity of the interpolants. To overcome these drawbacks, the higher-order stiffness term can be recast as a higher-order inertia term by using Padé approximations or other mathematical manipulations. The model of Eq. (1) thus results.

Other motivations for higher-order inertia are possible as well [4–9]. In this contribution we do not investigate the physical backgrounds further of such models, but instead focus on the aspects of discretisation in space and in time. In Section 2, we investigate how the critical time step in the Newmark time integration algorithm is affected by the additional inertia. Furthermore, based on a dispersion analysis of the space–time discretised medium we provide guidelines in Section 3 on how to choose time step and finite element size. We will employ linear finite elements and the Newmark scheme throughout, while uniform element lengths h and uniform time step sizes Δt will also be assumed. This will then enable us to provide recommendations on selection of the element size and the time step.

2. Stability aspects: critical time step

After spatial discretisation, the element equations according to Eq. (1) can be written as [10]

$$[\mathbf{M} + \mathbf{M}_{\mathrm{m}}]\ddot{\mathbf{d}} + \mathbf{K}\mathbf{d} = \mathbf{f}, \tag{3}$$

where the various element matrices are given as

$$\mathbf{M} = \rho h \begin{bmatrix} \frac{1}{3} & \frac{1}{6} \\ \frac{1}{6} & \frac{1}{3} \end{bmatrix}, \quad \mathbf{M}_{\mathrm{m}} = \frac{\rho\ell^2}{h} \begin{bmatrix} 1 & -1 \\ -1 & 1 \end{bmatrix}, \quad \mathbf{K} = \frac{E}{h} \begin{bmatrix} 1 & -1 \\ -1 & 1 \end{bmatrix}. \tag{4}$$

Furthermore, $\mathbf{d}$ is a vector with the nodal displacements and $\mathbf{f}$ is a vector that contains the contributions of boundary tractions and body forces. For the time integration explicit algorithms (such as the central difference scheme) or implicit algorithms (such as the Newmark scheme) can be used. All explicit algorithms and some implicit algorithms are only conditionally stable, that is, the applied time step must be selected smaller than a so-called *critical time step* in order for the simulations to remain numerically stable.

In order to derive the critical time step for the Newmark algorithm, we employ the strategy set out by Hughes [11], that is,

$$\Delta t_{\mathrm{crit}} = \frac{\Omega_{\mathrm{crit}}}{\omega_{\max}}, \tag{5}$$

where Δt_{crit} is the sought critical time step, $\Omega_{\mathrm{crit}} = 1/\sqrt{\gamma/2 - \beta}$ is the critical sampling frequency of the Newmark scheme and $\omega_{\max}$ is the maximum angular frequency that can be captured by the applied spatial discretisation. The Newmark parameters γ and β set the accuracy, stability and numerical damping of the time integration scheme. The maximum angular frequency $\omega_{\max}$ is obtained by solving the homogeneous equivalent of Eq. (3), which results in the following eigenvalue problem:

$$\det[-\omega^2(\mathbf{M} + \mathbf{M}_{\mathrm{m}}) + \mathbf{K}] = 0. \tag{6}$$

Using the definitions given in Eq. (4), the eigenvalue problem can be solved in terms of ω as

$$\omega = \frac{c_e\sqrt{12}}{h}\frac{1}{\sqrt{1+12(\ell/h)^2}} \tag{7}$$

in which $c_e = \sqrt{E/\rho}$ is the elastic wave velocity in 1D systems. Thus,

$$\Delta t_{\text{crit}} = \frac{h}{c_e\sqrt{12(\gamma/2-\beta)}}\sqrt{1+12(\ell/h)^2}, \tag{8}$$

which is expressed as the critical time step for classical elasticity (retrieved through $\ell = 0$) times a magnification factor due to the higher-order inertia.

This is illustrated for the Fox–Goodwin scheme which is retrieved from the Newmark scheme by taking $\gamma = \frac{1}{2}$ and $\beta = \frac{1}{12}$. Wave propagation through a bar of length 100 m is studied numerically with the material parameters $c_e = 1\,\text{m/s}$ and $\ell = 1\,\text{m}$. The bar is loaded with a unit pulse at the left end. Taking the element size $h = 1\,\text{m}$, the critical time step is computed from Eq. (8) as $\Delta t_{\text{crit}} = 2.5495\,\text{s}$. The simulations are run till time

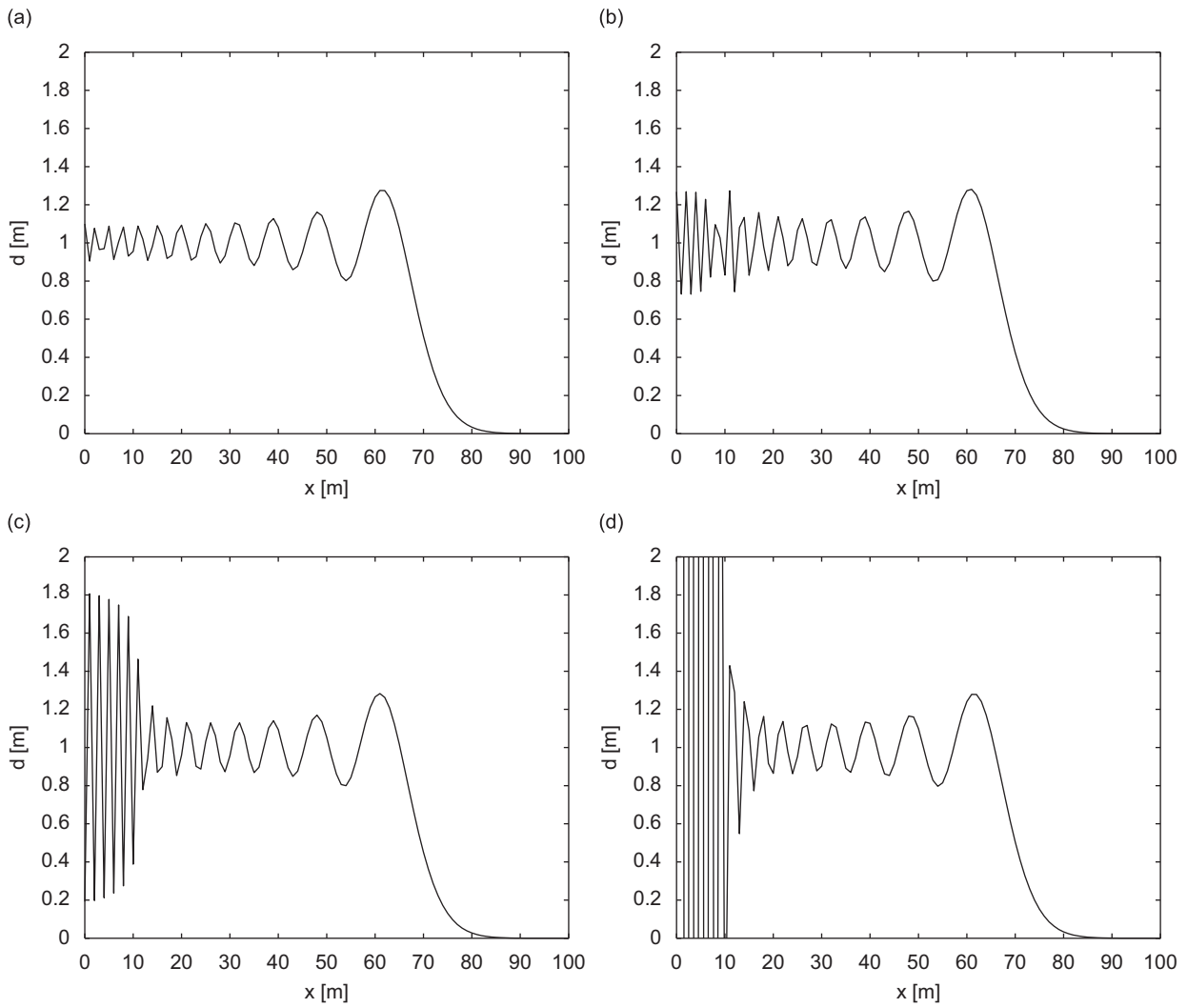

Fig. 1. Role of critical time step $\Delta t_{\text{crit}} = 2.5495\,\text{s}$ in the Fox–Goodwin scheme—displacement profiles along bar for applied time step $\Delta t = 2\,\text{s}$ (a), $\Delta t = 2.54\,\text{s}$ (b), $\Delta t = 2.55\,\text{s}$ (c) and $\Delta t = 2.57\,\text{s}$ (d).

$t = 74$ s with different time steps, both below and above the critical time step. The final profiles of the displacements along the bar are shown in Fig. 1. Taking a time step $\Delta t = 2$ s well below Δt_{crit} results in a displacement profile without artificial amplification of oscillations. With $\Delta t = 2.54$ s the time step is just below Δt_{crit}; while some amplification of the higher frequencies takes place, their amplitude nevertheless remains bounded. If the time step $\Delta t = 2.55$ s is just above Δt_{crit}, the higher frequencies are amplified and start to dominate the rest of the response. Finally, taking $\Delta t = 2.57$ s the high-frequency oscillations grow with every time step and become unbounded. Note that for this model with higher-order inertia the lower frequencies are not affected by the additional mass term, but the higher frequencies are slowed down. Thus, it is exactly these higher frequencies which are destabilised first if the selected time step results in a too large enforced propagation of the wave.

3. Accuracy aspects: discrete dispersion relation

The dispersion relation after discretisation in space and time will be derived next. After assembly of the element equations of expression (3), the nth equation reads

$$\frac{1}{6}\rho h(a_{n-1} + 4a_n + a_{n+1}) + \frac{\rho \ell^2}{h}(-a_{n-1} + 2a_n - a_{n+1}) + \frac{E}{h}(-d_{n-1} + 2d_n - d_{n+1}) = 0, \tag{9}$$

where a_n is the time-discretised acceleration of node n. Eq. (9) contains terms with accelerations and with displacements, the latter of which are of the simpler format. Therefore, it is most convenient to eliminate the displacements from the formulation. To this end, three consecutive time instants with constant time step Δt will be considered. The standard Newmark equations relate time step t^{j+1} to time step t^j, that is [11]

$$d^{j+1} = d^j + \Delta t v^j + (\tfrac{1}{2} - \beta)\Delta t^2 a^j + \beta \Delta t^2 a^{j+1}. \tag{10}$$

Furthermore, the Newmark equations relating time step t^{j-1} to time step t^j can be used to derive that

$$d^{j-1} = d^j - \Delta t v^j + (\tfrac{1}{2} - \gamma + \beta)\Delta t^2 a^{j-1} + (\gamma - \beta)\Delta t^2 a^j. \tag{11}$$

For an objective assessment of the dispersive properties of the continuum model, it is appropriate to eliminate numerical damping from the description. Hence, the Newmark parameter γ should be taken as $\gamma = \frac{1}{2}$. It then follows from Eqs. (10) and (11) that

$$d^{j-1} - 2d^j + d^{j+1} = \beta \Delta t^2 a^{j-1} + (1 - 2\beta)\Delta t^2 a^j + \beta \Delta t^2 a^{j+1}. \tag{12}$$

Next, Eq. (9) is evaluated at time t^{j+1} (multiplied with -1), at time t^j (multiplied with 2) and at time t^{j-1} (multiplied with -1). Adding these three expressions and introducing the dimensionless element size h/ℓ and the dimensionless time step $c_e \Delta t/\ell$ gives

$$\begin{aligned}
&\frac{1}{6}\frac{h^2}{\ell^2}(a_{n-1}^{j-1} + 4a_n^{j-1} + a_{n+1}^{j-1} - 2a_{n-1}^{j} - 8a_n^{j} - 2a_{n+1}^{j} + a_{n-1}^{j+1} + 4a_n^{j+1} + a_{n+1}^{j+1}) \\
&\quad + (-a_{n-1}^{j-1} + 2a_n^{j-1} - a_{n+1}^{j-1} + 2a_{n-1}^{j} - 4a_n^{j} + 2a_{n+1}^{j} - a_{n-1}^{j+1} + 2a_n^{j+1} - a_{n+1}^{j+1}) \\
&\quad + \beta\frac{c_e^2 \Delta t^2}{\ell^2}(-a_{n-1}^{j-1} + 2a_n^{j-1} - a_{n+1}^{j-1} - a_{n-1}^{j+1} + 2a_n^{j+1} - a_{n+1}^{j+1}) \\
&\quad + (1 - 2\beta)\frac{c_e^2 \Delta t^2}{\ell^2}(-a_{n-1}^{j} + 2a_n^{j} - a_{n+1}^{j}) = 0,
\end{aligned} \tag{13}$$

where Eq. (12) has been used to eliminate the displacements d. For the discretised system a solution of the form $a_n^j = A\exp(\mathrm{i}(kx_n - \omega t_j))$ is used. With uniform step sizes h and Δt in space and time it holds that $x_n = nh$ and $t_j = j\Delta t$, by which $a_n^j = A\exp(\mathrm{i}(knh - \omega j \Delta t))$. Moreover, $a_{n\pm1}^{j\pm1} = a_n^j \exp(\pm \mathrm{i}kh)\exp(\mp \mathrm{i}\omega \Delta t)$. Eq. (13) can

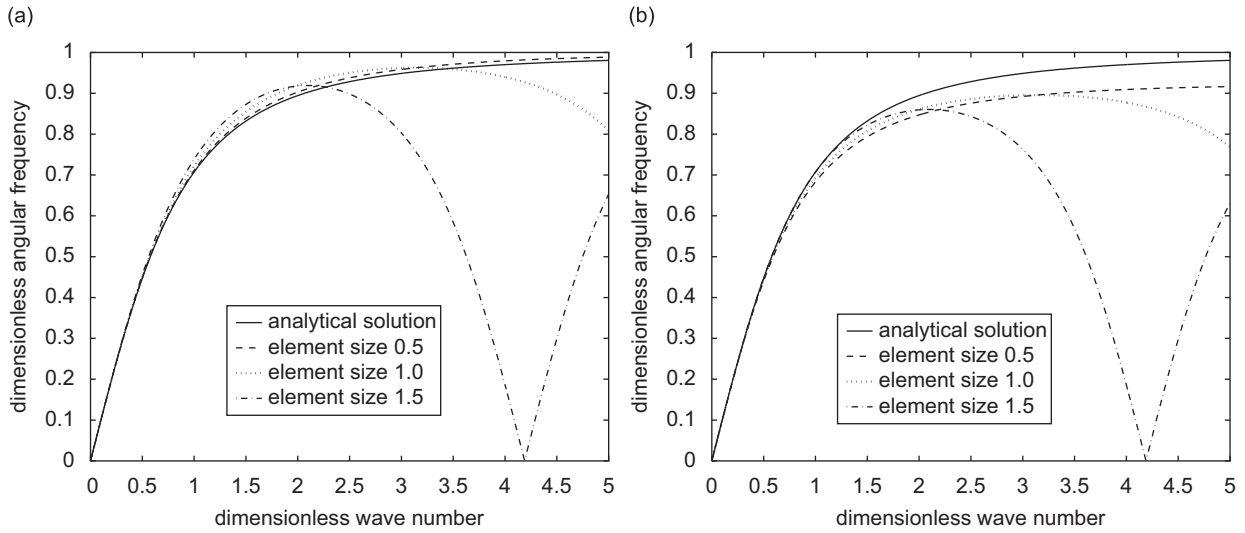

Fig. 2. Angular frequency versus wavenumber—Fox–Goodwin scheme with $\beta = \frac{1}{12}$ (a) and average acceleration scheme with $\beta = \frac{1}{4}$ (b).

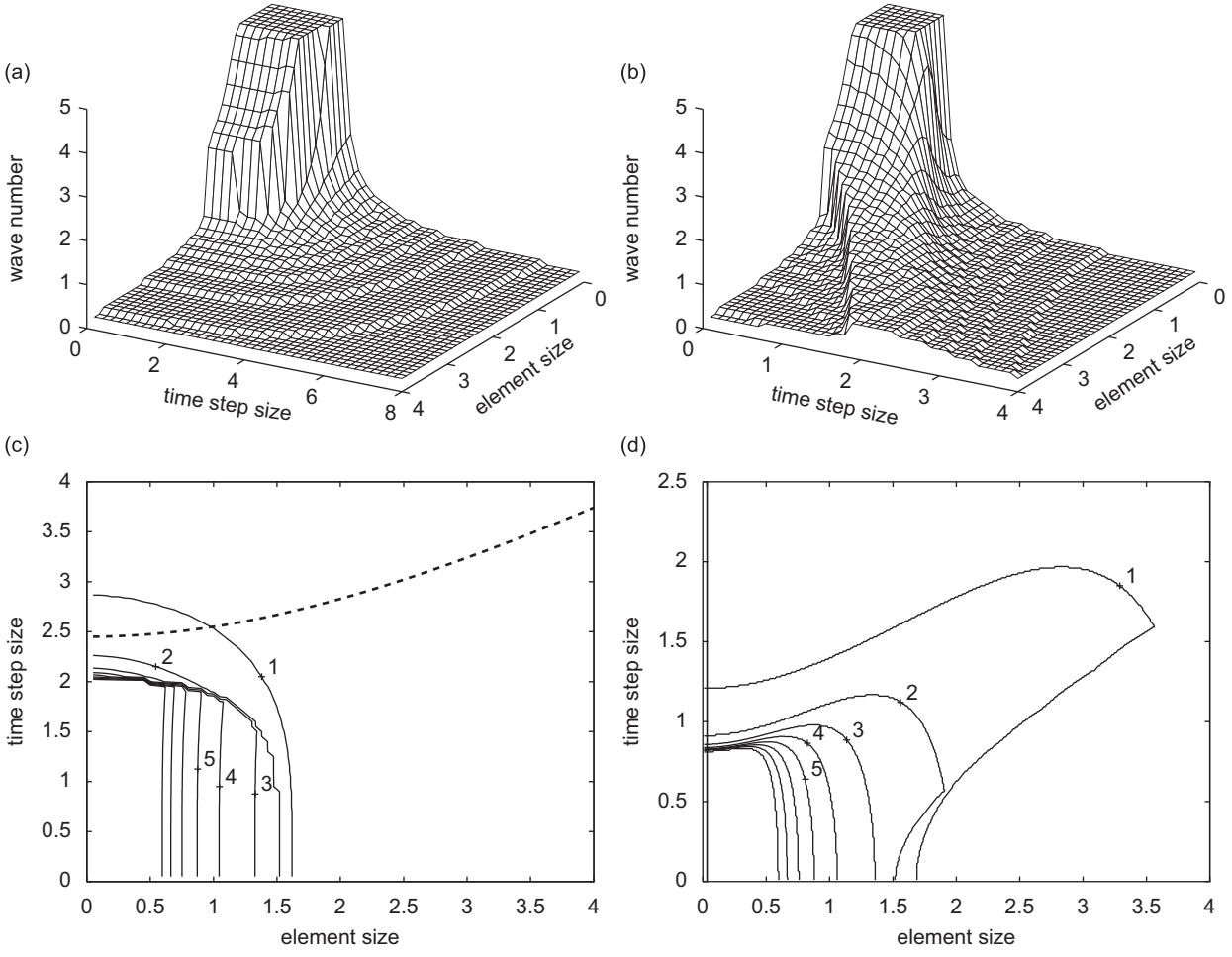

Fig. 3. 3D plots and contour plots of wavenumbers with up to 5% error versus dimensionless element size and dimensionless time step—Fox–Goodwin scheme (a/c) and average acceleration scheme (b/d); the critical time step according to Eq. (8) is indicated with a dashed line.

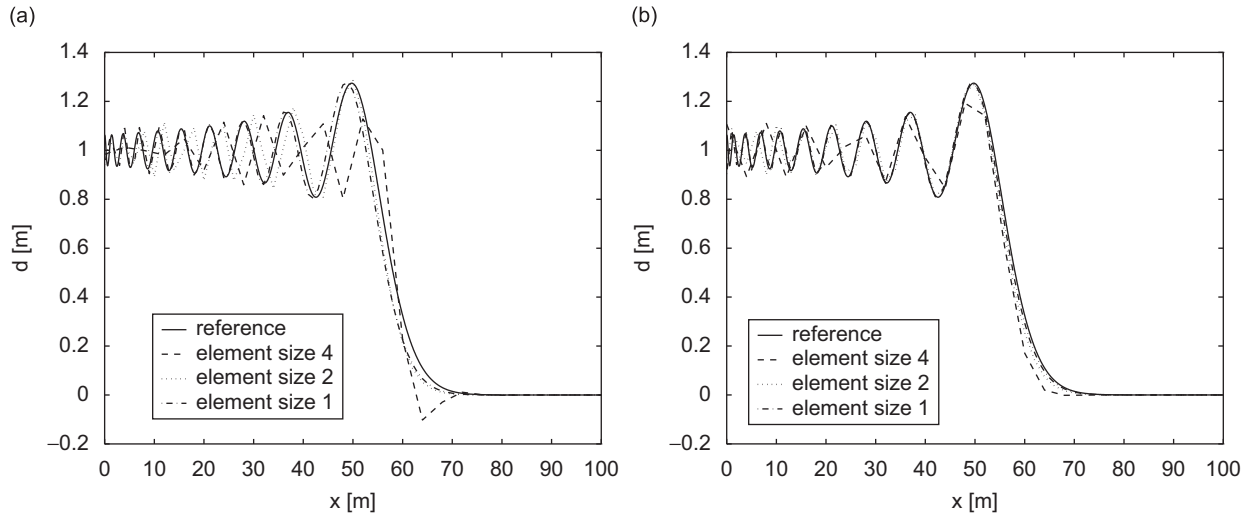

Fig. 4. Wave profiles for Fox–Goodwin scheme (a) and average acceleration scheme (b).

then be rewritten as

$$2\cos(\omega\Delta t)\left[2\cos(kh)\left\{\frac{1}{6}\frac{h^2}{\ell^2}-1-\beta\frac{c_e^2\Delta t^2}{\ell^2}\right\}+\frac{2}{3}\frac{h^2}{\ell^2}+2+2\beta\frac{c_e^2\Delta t^2}{\ell^2}\right]$$
$$=2\cos(kh)\left\{\frac{1}{3}\frac{h^2}{\ell^2}-2+(1-2\beta)\frac{c_e^2\Delta t^2}{\ell^2}\right\}+\frac{4}{3}\frac{h^2}{\ell^2}+4-(2-4\beta)\frac{c_e^2\Delta t^2}{\ell^2}, \tag{14}$$

which can be used to resolve the angular frequency ω as a function of the wavenumber k.

In Fig. 2 we have evaluated the dimensionless angular frequency $\omega\ell/c_e$ against the dimensionless wavenumber $k\ell$ as computed from Eq. (14) for two variants of the Newmark scheme, namely the conditionally stable Fox–Goodwin scheme ($\beta=\frac{1}{12}$) and the unconditionally stable average acceleration scheme ($\beta=\frac{1}{4}$). Furthermore, $c_e\Delta t/\ell=1$ and three different values for h/ℓ have been taken. The analytical solution for the angular frequency has also been plotted, by which the influence and the accuracy of the numerical discretisation can be assessed a priori. As a next step, for a range of element sizes and for a range of time steps we have computed the minimum wavenumber for which the angular frequency deviates more than 5% from the analytical solution. The results are shown in Fig. 3, both in a three-dimensional representation and in a more quantitative contour plot (note that the axes ranges are not the same for each plot). These plots can facilitate the choice of the numerical discretisation parameters. Firstly, however, the analyst must select the range of wavenumbers that need to be simulated accurately. For the Fox–Goodwin scheme it follows that a dimensionless time step of magnitude 1.5–2.0 is adequate for a large range of dimensionless element sizes. For the average acceleration scheme, taking $c_e\Delta t/\ell\approx\frac{1}{2}h/\ell$ provides efficient discretisations, by which it follows that the optimal time step $\Delta t\approx\frac{1}{2}h/c_e$ for a wide range of values for the microstructural length ℓ.

To illustrate these findings, the example of Section 2 is revisited. All parameters are the same as before unless mentioned otherwise. The wave profile at time $t=60\,\mathrm{s}$ is investigated, and a reference solution is computed using 1000 finite elements over the bar length and a time step size $\Delta t=0.1\,\mathrm{s}$. We have used values of the dimensionless element size $h/\ell\in[1,2,4]$ and we have used the two recommendations to link time step to element size for the two variants of the general Newmark scheme. The resulting wave profiles are shown in Fig. 4. It can be seen that both variants of the Newmark scheme show a good convergence upon mesh refinement towards the reference solution. Taking the dimensionless element size $h/\ell=1$ seems to be an appropriate choice for describing the wave front of pulse loads, indicating that dimensionless wavenumbers up to $k\ell\approx4$ are relevant. If coarser discretisations are necessary, the Fox–Goodwin scheme offers good accuracy for relatively large time steps combined with small elements, whereas the average acceleration scheme offers good accuracy for moderately large elements combined with proportionally scaled time steps.

4. Conclusions

In this short note, we have studied two discretisation aspects of a continuum theory enriched with higher-order inertia. The higher-order inertia term is a representation of the underlying microstructure and it is accompanied by a coefficient in terms of an internal length scale. The stability limit in terms of a critical time step has been derived for the relevant variants of the Newmark scheme; this has also been illustrated numerically for the conditionally stable Fox–Goodwin scheme. It was found that the critical time step increases due to the presence of the higher-order inertia. Furthermore, if the time step is taken too large (that is, larger than the critical time step), destabilising effects are first observed for the higher frequencies.

Next, recommendations on the finite element size and the time step have been derived using a discrete dispersion analysis. After determining a range of wavenumbers that must be described accurately, first a suitable element size and then a suitable time step can be selected. We found that taking the element size more or less equal to the microstructural length scale parameter gives a good accuracy for a wide range of wavenumbers. Taking smaller element sizes is of course possibly but would then raise the question whether it may be more efficient to model the microstructure explicitly rather than via higher-order inertia.

References

[1] M.B. Rubin, P. Rosenau, O. Gottlieb, Continuum model of dispersion caused by an inherent material characteristic length, *Journal of Applied Physics* 77 (1995) 4054–4063.

[2] W. Chen, J. Fish, A dispersive model for wave propagation in periodic heterogeneous media based on homogenization with multiple spatial and temporal scales, *ASME Journal of Applied Mechanics* 68 (2001) 153–161.

[3] I.V. Andrianov, J. Awrejcewicz, R.G. Barantsev, Asymptotic approaches in mechanics: new parameters and procedures, *ASME Applied Mechanics Reviews* 56 (2003) 87–110.

[4] E.C. Aifantis, On the role of gradients in the localization of deformation and fracture, *International Journal of Engineering Science* 30 (1992) 1279–1299.

[5] I. Vardoulakis, E.C. Aifantis, On the role of microstructure in the behavior of soils: effects of higher order gradients and internal inertia, *Mechanics of Materials* 18 (1994) 151–158.

[6] Z.-P. Wang, C.T. Sun, Modeling micro-inertia in heterogeneous materials under dynamic loading, *Wave Motion* 36 (2002) 473–485.

[7] A.V. Metrikine, H. Askes, One-dimensional dynamically consistent gradient elasticity models derived from a discrete microstructure. Part 1: generic formulation, *European Journal of Mechanics A/Solids* 21 (2002) 555–572.

[8] J. Engelbrecht, A. Berezovski, F. Pastrone, M. Braun, Waves in microstructured materials and dispersion, *Philosophical Magazine* 85 (2005) 4127–4141.

[9] G.W. Milton, J.R. Willis, On modifications of Newton's second law and linear continuum elastodynamics, *Proceedings of the Royal Society A* 463 (2007) 855–880.

[10] J. Fish, W. Chen, G. Nagai, Non-local dispersive model for wave propagation in heterogeneous media: one-dimensional case, *International Journal for Numerical Methods in Engineering* 54 (2002) 331–346.

[11] T.J.R. Hughes, *The Finite Element Method: Linear Static and Dynamic Finite Element Analysis*, Dover, 2000.